

Water Modeled Signal Removal and Data Quantification in Localized MR Spectroscopy Using a Time-Scale Postacquisition Method

Haçène Serrai,* Lotfi Senhadji,† David B. Clayton,‡ Chun Zuo,* and Robert E. Lenkinski*

*Beth Israel Deaconess Medical Center, Harvard Medical School, Boston, Massachusetts 02215; †Laboratoire Traitement du Signal et de l'Image (LTSI), INSERM EMI 9934, Université de Rennes 1, Rennes 35042 Cedex, France; and ‡Department of Radiology, University of Pennsylvania, School of Medicine, Philadelphia, Pennsylvania 19104

Received August 2, 2000; revised January 10, 2001

We have previously shown the continuous wavelet transform (CWT), a signal-processing tool, which is based upon an iterative algorithm using a lorentzian signal model, to be useful as a postacquisition water suppression technique. To further exploit this tool we show its usefulness in accurately quantifying the signal metabolites after water removal. However, due to the static field inhomogeneities, eddy currents, and "radiation damping," the water signal and the metabolites may no longer have a lorentzian lineshape. Therefore, another signal model must be used. As the CWT is a flexible method, we have developed a new algorithm using a gaussian model and found that it fits the signal components, especially the water resonance, better than the lorentzian model in most cases. A new framework, which uses the two models, is proposed. The framework iteratively extracts each resonance, starting by the water peak, from the raw signal and adjusts its envelope to both the lorentzian and the gaussian models. The model giving the best fit is selected. As a consequence, the small signals originating from metabolites when selecting, removing, and quantifying the dominant water resonance from the raw time domain signal are preserved and an accurate estimation of their concentrations is obtained. This is demonstrated by analyzing (^1H) magnetic resonance spectroscopy unsuppressed water data collected from a phantom with known concentrations at two different field strengths and data collected from normal volunteers using two different localization methods. © 2001 Academic Press

Key Words: localized magnetic resonance spectroscopy; continuous wavelet transform; water suppression; quantification.

1. INTRODUCTION

The development of localized *in vivo* proton (^1H) spectroscopic methods has involved the suppression of the water resonance using a variety of approaches, which may be divided into two general categories. The first category, called preacquisition methods (1–4), includes reducing the longitudinal and transverse water magnetization using CHESS pulses followed by spoiler gradients (5) or applying a frequency selective inversion pulse to the water resonance and choosing a preacquisition delay such that the water resonance is passing through null (6). Other methods, which avoid the excitation of the water spins (7), or methods based on T_2 differences (8) may be used. These approaches were

based on the premise that the analog to digital converter had insufficient dynamic range to accurately digitize small metabolite signals (1–10 mM) in the presence of the dominant water (approximately 80 M). Water suppression from the acquired free induction decay (FID) allows observation of the signals arising from these dilute metabolites. In these methods the accuracy of data analysis, especially metabolite quantification, may depend upon the quality and the degree of water suppression.

The performance of most of these preacquisition methods depends on a number of technical issues such as the frequency profile and phase of the selective pulses and the homogeneities of the radiofrequency and B_0 fields. As a result, the spectrum may suffer from incomplete solvent suppression, baseline distortions, artifacts, and the partial saturation of signals close to the water resonance (9). Furthermore, the magnetic interactions, such as dipolar coupling, between water and the metabolites detected in the brain and muscle may be affected, leading to an underestimation of the metabolite concentrations when using the preacquisition methods (10).

The advent of high-speed receivers capable of oversampling (11) and the improvements in the analogue to digital converters have increased the dynamic range of the receiver. This increase allows sampling of the signal of the small metabolites in the presence of a strong water component. This still leaves the problem of removing the water in the processing of the data. A second category of water suppression techniques, called postacquisition methods, has emerged (12–17) which can address this problem. These methods employ different mathematical approaches to remove the water component from the magnetic resonance spectroscopy (MRS) data. These algorithms are based on bandpass filtering in the time or frequency domains (12, 13), data matrix representation using singular value decomposition or Toeplitz matrix decomposition (14, 15), or fitting the water peak by means of a nonlinear least-squares method (16). The postacquisition methods allow quantification of the water peak, which can then be used as an internal reference for frequency, linewidth, and concentration (18). Time-frequency and time-scale approaches, such as continuous wavelet transforms (CWT), have been proposed as postacquisition methods in order to remove the water

peak from the unsuppressed solvent data (19, 20) and for accurate quantification of MRS metabolite signals based on the lorentzian model (21). This method is based on an iterative process which extracts, quantifies, and subtracts the signal components from the raw signal sequentially, according to their respective apparent relaxation time (T_2^*) values. The extraction of the signal components is based on their time duration rather than their magnitudes.

Although the postacquisition methods do not suffer from the problems associated with preacquisition methods, they present their own set of challenges. In particular, they can be sensitive to interactions, which result in a non-lorentzian lineshape for the water resonance. Furthermore, few of the proposed postacquisition methods described in the literature went beyond the suppression of the water peak to accurately quantify the remaining metabolite components.

The aim of this paper is to overcome the lineshape peaks problem and to propose a new global framework for absolute quantification of unsuppressed water signal data using CWT. Therefore, the following points are addressed:

(i) theory developments of the extension of the previous CWT method to the quantification of MRS data signals based on the gaussian model (Section 2);

(ii) application of the new framework to water signal suppression and absolute quantification of metabolites, in *in vitro* and *in vivo* unsuppressed water MRS data, modeled as an unknown mixture of gaussian and lorentzian signals (Sections 3 and 4).

Results of two studies are reported.

(1) The first consists of analyzing proton data acquired without water suppression from a phantom containing metabolites with known concentrations on different scanners (Siemens and General Electric) using two different localization techniques (PRESS and STEAM).

(2) The second study consists of quantifying *in vivo* unsuppressed water proton spectra obtained from normal volunteers and comparing the results of the quantitation of the metabolites to the results obtained from the *in vivo* proton data acquired with water suppression. The aim of these studies is to determine the accuracy of unsuppressed proton MRS in terms of absolute metabolite concentrations in phantoms and relative concentrations in volunteers.

2. METHOD FOR QUANTIFICATION OF THE UNSUPPRESSED WATER MRS DATA

The CWT analyzes a nonstationary signal by transforming its input time domain into a time-scale domain (22). Through translation and dilation operations, the CWT decomposes the signal according to a set of functions deduced from a defined prototype function, assumed to be well localized in both time and frequency domains.

In mathematical terms, the CWT of a signal of finite energy with respect to the defined prototype function $g(t)$ in the time domain is given by

$$S_a(b) = \langle s, g_{a,b} \rangle = \int s(t) \cdot g_{a,b}^*(t) \cdot dt, \quad [1]$$

with $g_{a,b}(t) = \frac{1}{a}g(\frac{t-b}{a})$, characterized by two parameters, the scale or dilation parameter noted a ($a > 0$) and the translation parameter noted b ($b \in R$). The asterisk stands for the complex conjugate. Any prototype function $g(t)$ belonging to $L^2(R)$ is called an analyzing wavelet if it complies with the so-called admissibility condition (23). The transform in Eq. [1] maps the signal via a two-dimensional function $S_a(b)$ on the time-scale domain plane (a, b). This operation is equivalent to a particular filter-bank analysis in which the relative frequency bandwidths ($\Delta\omega/\omega$) are constant and related to the parameters a, b and to the frequency properties of the wavelet g . To achieve a correct analysis of the signal $s(t)$, regularity and suitable time-frequency bandwidth product are required for g . The most commonly used analyzing wavelet has been the so-called Morlet wavelet (22, 23):

$$g(t) = e^{(-t^2/2)} \cdot e^{(i\omega_0 t)} + c(t), \quad [2]$$

where $c(t)$ is a correction term to enforce the admissibility condition. For $\omega_0 > 5$, the term $c(t)$ is numerically negligible and $g(t)$ is practically applicable (24). Due to the causality of the MRS signal ($s(t) \in R^+$), the translation parameter is positive, $b \in R^+$. The CWT method has been proposed to quantify the time domain MRS data with a lorentzian model (21). The details of the developed iterative procedure given elsewhere (25) are briefly summarized here.

Consider $s(t)$ a noise-free FID signal composed of one damped complex sinusoid given by

$$s(t) = A \cdot e^{(-t/T_2^*)} \cdot e^{i(\omega_s t + \varphi)}, \quad [3]$$

where T_2^* and $\omega_s = 2\pi\delta_s$ are the apparent relaxation time and the angular frequency (chemical shift δ_s), respectively, of the signal s .

Substituting $s(t)$ and $g(t)$ for Eqs. [3] and [2], respectively, in Eq. [1] and referring to (21, 25), the CWT of $s(t)$ is given by

$$S_{a_r}(b) = A \cdot \sqrt{\frac{\pi}{2}} [1 \mp \sqrt{1 - e^{-\alpha^2}}] \cdot e^{\left(\frac{a_r^2 - 2bT_2^*}{2T_2^{*2}}\right)} \cdot e^{i(\omega_s b + \varphi)}, \quad [4]$$

where a_r is the final dilation parameter value obtained at the convergence of the used iterative algorithm (21, 25), with $\alpha = [(a_r/T_2^*) - (b/a_r)]$ and the signs \mp are conditioned by the sign of α . A simple nonlinear regression algorithm applied on the modulus of Eq. [4] provides the values of A and T_2^* , whereas the angular frequency ω_s and phase φ are linearly estimated from the phase of $S_{a_r}(b)$. The latter is equal to the signal $s(t)$ at every

point $t = b$ up to a known function $F(b)$ given by

$$F(b) = \sqrt{\frac{\pi}{2}} e^{(a_r^2/2 \cdot T_2^{*2})} \left[1 \mp \sqrt{1 - e^{-\alpha^2}} \right]. \quad [5]$$

In a general case where the signal $s(t)$ is composed of N ($N > 1$) components, the resonances are successively extracted, quantified according to their time duration (T_2^*) in a decreasing order, and subtracted with respect to the corresponding function $F_{j,j=1,N}(b)$ from the raw signal in an iterative process. The signal component $s_{j,j=1,N}$ possessing the greatest T_2^* value is quantified first. With an appropriate choice of the translation parameter b , its corresponding resonance frequency ($\omega_{j,j=1,N}$) is estimated at the end of the FID signal. The above signal component is then extracted, quantified, and subtracted from the raw signal (see details in Ref. 21).

The developed iterative procedure above has been tested in quantifying and removing the water peak modeled as a complex exponential decay in ^1H MRS time-domain data without water suppression (20). The CWT was able to suppress the water peak without affecting the small metabolite components close to it. This is performed by a frequency bandwidth reduction achieved by an increase of the value of a_r (21). We extend here the water peak removal by analyzing the remaining metabolite signals and obtaining an estimation of their absolute concentrations. However, we found experimentally that the signal components especially the water resonance in the proton data without suppression of the water may have a gaussian lineshape. We suggest that the main reason is due to the static field inhomogeneities.

As presented above, if the resonance frequency and the phase of the signal components are linearly calculated from the phase of Eq. [4] by CWT, the estimation of the amplitude and the apparent relaxation time values are signal model dependent. For an accurate estimation of the remaining parameters (A , T_2^*), the adapted signal model must be used. For this purpose, the method is extended here to quantify MRS signal with the gaussian envelope. Therefore, applying CWT, with the Morlet wavelet as a prototype function, to an FID signal of the form

$$s(t) = A \cdot e^{(-t^2/2 \cdot T_2^{*2})} \cdot e^{i \cdot (\omega_s \cdot t + \varphi)}, \quad [6]$$

and after some mathematical development inspired from (21) and following steps similar to those above, leads to

$$S_{a_r}(b) = A \cdot \sqrt{\frac{\pi \cdot T_2^*}{2 \cdot (T_2^* + a_r^2)}} \left[1 + \sqrt{1 - e^{-\alpha^2}} \right] \cdot e^{-b^2/2(T_2^* + a_r^2)} \cdot e^{i(\omega_s b + \varphi)}, \quad [7]$$

where a_r is the final dilation parameter value obtained at the convergence of the used iterative algorithm and $\alpha = \frac{-b \cdot T_2^*}{a_r^2 \cdot (T_2^* + a_r^2)}$. The values of A and T_2^* are nonlinearly estimated from the modulus whereas the angular frequency, ω_s , and phase, φ , are linearly calculated from the phase of $S_{a_r}(b)$. The function $F(b)$ in this

case becomes

$$F(b) = \sqrt{\frac{\pi \cdot T_2^*}{2 \cdot (T_2^* + a_r^2)}} \cdot e^{((b^2 \cdot a_r^2)/(2 \cdot T_2^* (T_2^* + a_r^2)))} \left[\sqrt{1 - e^{-\alpha^2}} \right]. \quad [8]$$

The decomposition product $S_{a_r}(b)$ is equal to the signal $s(t)$ at every point $t = b$ up to a known function $F(b)$. The same principle of sequential extraction and quantification of the signal components based on their time duration's holds as for the above lorentzian model.

3. MATERIALS AND METHODS

Two sets of ^1H MRS localized data without water suppression were collected from a 2.7-L spherical phantom. The first set consists of five FID signals acquired at 63.86 MHz on a 1.5-T scanner (Siemens Vision System, Iselin, NJ) with a PRESS sequence (TE = 40 ms, TR = 6 s, $2 \times 2 \times 2 \text{ cm}^3$ voxel size, 32 accumulations, 1 KHz spectral width, and 1 K data points). The second set contains four FID signals acquired at 170 MHz on a 4-T scanner (General Electric Medical Systems, Milwaukee, WI) with a STEAM sequence (TE = 30 ms, TR = 5 s, TM = 13.7 ms $2 \times 2 \times 2 \text{ cm}^3$ voxel size, 32 accumulations, ± 1250 Hz spectral width, and 1024 data points). Figures 1a and 1b display spectra of the aliphatic parts of unsuppressed water MRS signals acquired with STEAM and PRESS sequences, respectively. The phantom consists of 50 mM potassium phosphate monobasic, 56 mM sodium hydroxide, 12.5 mM *N*-acetyl-L-aspartic acid (NAA), 10 mM creatine hydrate, 3 mM choline chloride, 7.5 mM myo-inositol, 12.5 mM L-glutamic acid (monosodium salt), 5 mM DL-lactic acid (lithium salt), and 0.10% sodium azide. *In vivo* proton MRS localized brain data with and without water suppression were collected from a healthy volunteer on a Siemens whole body system (1.5 T) using a PRESS sequence with the same acquisition parameters as above. For the data acquired with water suppression, three CHESSE pulses were used to suppress the water resonance before signal acquisition. Prior to signal processing and quantification, the acquired signals were frequency demodulated by using an analytic solution to remove the spurious peaks added throughout the spectrum due to the acoustic vibrations of the gradients (28).

A new framework based on CWT is used to quantify the time-domain unsuppressed water signals, using a program developed in house, (Interactive Data Language, IRIX mipseb Ver. 5, Research Systems, Inc.) proceeding as follows.

For each signal component selected by the iterative procedure, the chemical shift value is estimated from the phase of $S_{a_r}(b)$, whereas the values of the amplitude A and relaxation time T_2^* are selected from the best fit of the modulus of $S_{a_r}(b)$ to the moduli of the signal models of Eqs. [4] and [7], which provide the signal component model.

Once the selected signal component is quantified, it is subtracted from the raw signal with the respect to the corresponding signal model function $F(b)$ of either Eq. [5] or Eq. [8]. The

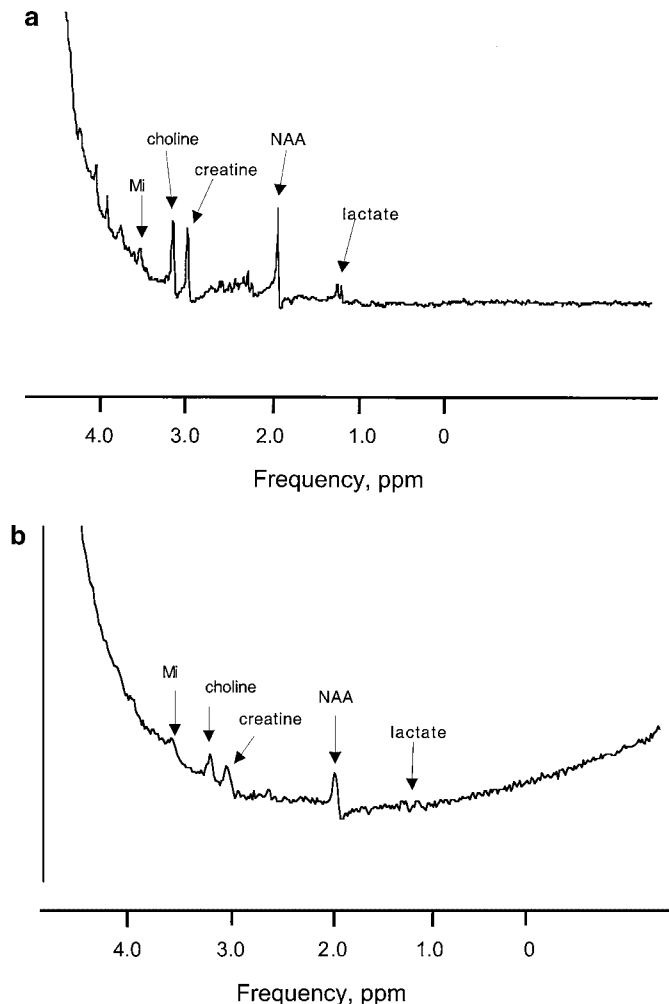


FIG. 1. (a) A spectrum of the aliphatic part of the MRS signal acquired without water suppression using the STEAM sequence at 4 T (TE = 30 ms, TR = 5 s, 1 K points, and 2500 Hz). (b) A spectrum of the aliphatic part of the MRS signal acquired without water suppression using the PRESS sequence at 1.5 T (TE = 40 ms, TR = 6 s, 1 K points, and 1000 Hz).

residue is used as an input signal to quantify another resonance for the next iteration.

In this scheme, the water peak is selected first, quantified, and subtracted from the raw signal. The adjacent metabolite signals are preserved by an appropriate increase of the dilation parameter value a_t during the use of the iterative procedure, reducing the frequency bandwidth of the time-frequency filter of the CWT. In the phantom studies, absolute concentration of the metabolites is obtained based on the concentration of the water (110 M).

4. RESULTS AND DISCUSSION

Figure 2a displays the spectrum of the aliphatic part of the residual signal after water peak subtraction by CWT from the signal shown in Fig. 1a. It qualitatively demonstrates that

the CWT removes the major part of the water resonance. The remaining water residue is removed by neglecting the first 16 points of the signal. This resulting signal is used to successively quantify the metabolite signals (Fig. 2b). For the Siemens data collected at 1.5 T the NAA, creatine, choline and myo-inositol peaks were quantified, whereas for the General Electric data collected at 4 T the myo-inositol peak is ignored. This is done because the myo-inositol peak is “deceptively simple” at 1.5 T and becomes a set of coupled peaks at 4 T, making it difficult to estimate it in the time domain by the CWT (29). The other

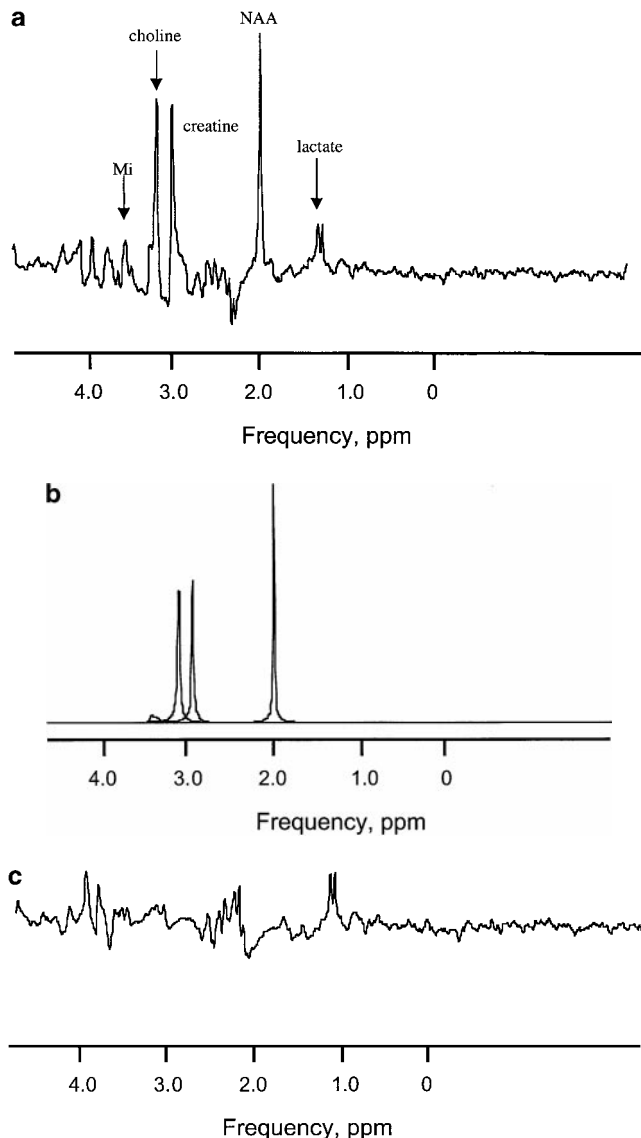


FIG. 2. (a) A spectrum of the same region as in Fig. 1a after water peak removal. Note the good quality of water peak suppression without alteration of the other metabolites and baseline distortion. The first 16 points are neglected from the signal residue after water resonance subtraction. (b) The sum of the peaks of NAA, creatine, choline, and myo-inositol successively extracted by the CWT method. (c) The final residue after subtraction of the metabolite peaks.

TABLE 1

Estimated Absolute Concentrations of the Metabolites (NAA, Creatine, Choline, and Myo-inositol) Obtained from Data Acquired using STEAM and PRESS Sequences and Their Errors

Metabolite		Estimated absolute concentration (mean value in mmol)		Percentage of the expected value \pm standard deviation	
		PRESS	STEAM	PRESS	STEAM
NAA	(12.5)	12.25	12.40	98 \pm 2.3	99.3 \pm 1.0
Creatine	(10)	9.34	9.45	93.4 \pm 3.8	94.5 \pm 2.1
Choline	(3)	2.78	2.78	92.6 \pm 3.4	92.7 \pm 8.5
Myo-inositol	(7)	6.83	—	91 \pm 7.7	—

Note. The true absolute concentration values are given in bold type.

metabolite peaks, such as the other creatine resonance, the lactate and the glutamate peaks, could be selected and quantified. We focus only on the major ones (NAA, creatine, choline, and myo-inositol). Furthermore, the CWT has been successfully tested in extracting and quantifying peaks from *in vivo* proton MRS brain data (25). The water peak either from Siemens (PRESS) or General Electric (STEAM) was gaussian. This was also true for the NAA and myo-inositol. For creatine and choline, the lorentzian model fits better than the gaussian model in the General Electric data, and the inverse is observed in the Siemens data.

The removal of the first data points does not affect the estimation of the MRS parameter values, especially the amplitudes. The correct amplitude values could be recovered. Let's assume that the portion of the MRS signal $s(t)$ belonging to $[0, T]$ is removed. The envelope of the resulting signal $s_T(t) = s(t + T)$; $t \geq 0$ is equal to $A_T \cdot e^{(-t^2/2 \cdot T_2^*)}$ for the gaussian model and to $A_T \cdot e^{(-t/T_2^*)}$ for the lorentzian model. Knowing the T value, which is equal to the number of the removed data points, the initial amplitude value is calculated from $A = A_T \cdot e^{(T^2/2 \cdot T_2^*)}$ (gaussian model), or $A = A_T \cdot e^{(T/T_2^*)}$ (lorentzian model). The equations above are used for a second time in a similar manner to correct for the amplitudes due to the T_2^* differences between the water and metabolites by substituting T to TE. The T value has

to be very small compared to the shortest T_2^* in the data in order to avoid a complete decrease of the corresponding metabolite component. The removal of the first 16 points would result in the inability to observe resonances that have T_2^* varying from 8 to 16 ms. Since in most of the processed data the T_2^* of the metabolite resonances are of the order of 75 ms or greater, wide accurate quantification should still be achievable after the removal of these first points. Quantification of macromolecules and lipids which have shorter T_2^* 's (i.e, broader lines) may be achieved in a better way if the first points are not removed (30).

The obtained results on the phantom data for the metabolite concentrations are reported in Table 1 for the PRESS and STEAM, respectively. The difference between the known metabolite concentration and its experimentally determined value increases as the metabolite's frequency becomes closer to that of water. This trend may reflect the fact that the accurate determination of these amplitudes may be sensitive to imperfections in the suppression of the water peak. Despite this trend, the accuracy of the obtained results is very good. The proposed method also provides an estimate of the apparent relaxation times (T_2^*) of the water and the metabolites. These values are summarized in Table 2 along with T_2 values reported by GE at 1.5 T. However, for all the signal components the obtained T_2^* values are underestimated compared to T_2 , except for the myo-inositol metabolite, which is overestimated by 3%. The main reason for this underestimation is the static field inhomogeneities, which deform the signal envelope, and the data length (1 K points), which may be too short to allow a complete acquisition of the signal. Less precision is observed on the T_2^* values of creatine (22.8% for PRESS and 4.2% for STEAM) and choline (15.4% for PRESS and 2.3% for STEAM) compared to NAA (7.5% for PRESS and 0.3% for STEAM). The lack of precision is mainly due to the overlap between creatine and choline peaks.

To further demonstrate the usefulness of the method, one *in vivo* spectrum without water suppression is analyzed and the relative ratios of the metabolite amplitudes are compared to those obtained from the *in vivo* spectrum with water suppression. The NAA/creatine and creatine/choline ratios observed in the suppressed spectrum are 2.8 and 1.9, respectively, whereas

TABLE 2

Estimated Apparent Relaxation Times T_2^* of the Signal Metabolites (NAA, Creatine, Choline, and Myo-inositol) and Water Resonance from Data Acquired Using STEAM and PRESS Sequences and the Errors to the True T_2 Values at 1.5 T

T_2 (1.5 T)		Estimated relaxation time (T_2^*) (mean value ms) \pm standard deviation (PRESS)	Estimated relaxation time (T_2^*) (mean value ms) \pm standard deviation (STEAM)
Water	(265)	212.2 \pm 3.9	193.6 \pm 0.2
NAA	(400)	223.6 \pm 7.5	202.5 \pm 1.1
Creatine	(265)	201.2 \pm 22.8	180.4 \pm 4.2
Choline	(175)	169.3 \pm 15.4	163.1 \pm 2.3
Myo-inositol	(75)	78.2 \pm 5.0	—

Note. The true T_2 values for the phantom are written in bold type and reported from the manufacturer (R. Hurd, General Electric, spectroscopy manual).

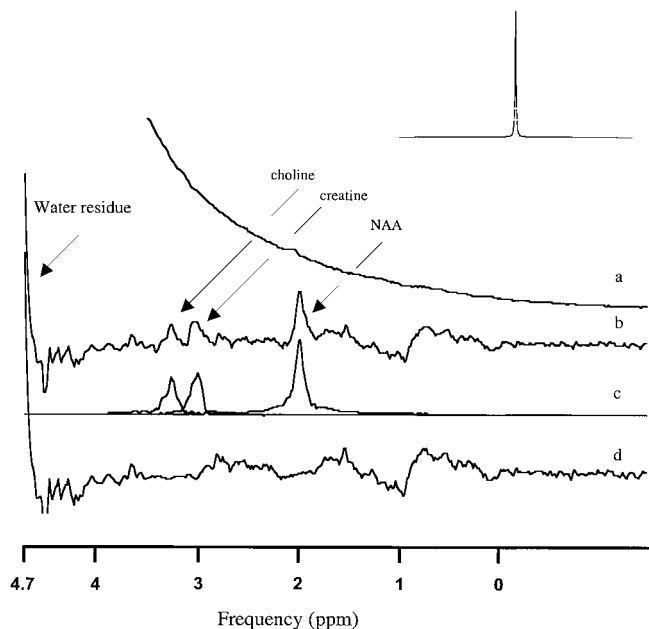


FIG. 3. (a) Magnified view of the aliphatic part of the *in vivo* spectrum shown in the inset acquired with PRESS sequence at 1.5 T (TE = 40 ms, TR = 6 s, 1 K points, and 1 kHz). (b) Spectrum of the same part as above after water signal suppression by CWT (LB = 3 Hz). (c) Peaks of the metabolites NAA, creatine, and choline extracted from the signal in (b) by CWT. (d) Difference between the spectra of (3b) and (3c) (LB = 3 Hz). (b), (c), and (d) are magnified 40 times compared to (a).

for the spectrum obtained without suppression of water they are 3.0 and 1.8. The error for both the NAA/creatine and the creatine/choline ratios is 6.2%, which is close to the sum of the standard deviations obtained from the phantom data of both creatine and choline, which is about 7%. Figure 3 displays spectra of the aliphatic part of the unsuppressed water *in vivo* data before and after water signal suppression and after subtraction of the metabolite peaks.

There is a drop in the SNR of water by 40 and 65 dB for the *in vivo* and the phantom data, respectively, when the water signal is removed by the proposed CWT scheme. The water is suppressed by about a factor of 10,000. The SNR of the NAA peak (*in vivo* data) in the CWT water suppressed spectrum is about 17:1, which is well above the SNR of MRS signals quantified elsewhere (21, 26, 27).

5. CONCLUSIONS

We have described a new framework based on the continuous wavelet transform approach for the quantification of MRS data without suppression of water acquired using localized spectroscopy techniques. Two signal model envelopes are included in the procedure, the classical lorentzian model and the newly added gaussian model. An automatic selection of the signal envelope model is obtained based on the best fit. This approach is tested on *in vitro* MRS data without water suppression to

obtain the absolute concentrations of the metabolites based on the estimation of the water content and relative concentrations from *in vivo* data. Furthermore, other signal models, such as multilorentzians and multigaussians, may be used if needed and could be easily implemented and added to the technique, showing its flexibility to analyze data with different models. As a consequence, the problems induced by the static field inhomogeneities, eddy currents, etc., are addressed.

Using this approach we have demonstrated that it is possible to acquire and quantify, without a significant loss of accuracy, localized MRS spectra with short TE without suppression of water. The accuracy of the results obtained from the spectra acquired on phantoms is excellent. The comparisons made between the results from the spectra obtained with and without water suppression on normal volunteer also show that good results can be attained from *in vivo* data without suppression of water.

ACKNOWLEDGMENTS

This study was sponsored by NIH grants RO1CA70362, RO1MH49390, RO1NS31464, and RR20305.

REFERENCES

1. P. J. Hore, in "Methods in Enzymology" (N. J. Oppenheimer and T. L. James, Eds.), p. 64, Academic Press, San Diego, 1989.
2. M. Guéron, P. Plateau, and M. Decors, Solvent signal suppression in NMR, *Prog. NMR Spectrosc.* **23**, 135–209 (1991).
3. M. Guéron and P. Plateau, in "Encyclopedia of Nuclear Magnetic Resonance" (D. M. Grant and R. K. Harris, Eds.), p. 4931, Wiley, New York, 1996.
4. V. Skelnár, in "NMR Applications in Biopolymers" (J. W. Finley, Ed.), p. 63, Plenum Press, New York, 1990.
5. I. M. Brereton, J. Field, L. N. Moxon, M. G. Irving, and D. M. Doddrell, Water suppression with B_0 field gradient homospoil pulses in high-resolution NMR spectroscopy, *Magn. Reson. Med.* **9**, 118–125 (1989).
6. R. J. Ogg, P. B. Kingsley, and J. S. Taylor, WET, a T_1 - and B_1 -insensitive water-suppression method for *in vivo* localized ^1H NMR spectroscopy, *J. Magn. Reson. B* **104**, 1–10 (1994).
7. J. R. Alger, A. Brunetti, G. Nagashima, and K. A. Hossmann, Evaluation of a newly discovered water suppression pulse sequence for high-field *in vivo* ^1H surface coil NMR spectroscopy, *Mag. Reson. Med.* **11**, 73–84 (1989).
8. D. L. Rabenstein, S. Fan, and T. T. Nakashima, Attenuation of the water resonance in Fourier transform ^1H NMR spectra of aqueous solutions by spin–spin relaxation, *J. Magn. Reson.* **64**, 541–546 (1985).
9. J. W. C. Van der Veen, D. R. Weinberger, J. A. Frank, and J. H. Duyn, Proton magnetic resonance spectroscopic imaging without water suppression, Proceedings of the VII ISMRM Meeting, Philadelphia, May, Vol. 1, p. 249 (1999).
10. R. A. De Graaf, R. Lamerichs, M. J. Kruijskamp, and K. Nicolay, Magnetic coupling between water and metabolites in human tissues, Proceeding of the VII ISMRM Meeting, Philadelphia, May, Vol. 1, p. 592 (1999).
11. M. A. Delsuc and J. Y. Lallemand, Improvement of dynamic range in NMR by oversampling, *J. Magn. Reson.* **69**, 504–507 (1986).
12. D. Marion, M. Ikura, and A. Bax, Improved solvent suppression in one- and two-dimensional NMR spectra by convolution of time-domain data, *J. Magn. Reson.* **84**, 425–430 (1989).

13. Y. Kuroda, A. Wada, T. Yamazaki, and K. Nagayama, Postacquisition data processing method for suppression of the solvent signal, *J. Magn. Reson.* **84**, 604–610 (1989).
14. G. Zhu, D. Smith, and Y. Hua, Post-acquisition solvent suppression by singular-value decomposition, *J. Magn. Reson.* **124**, 286–289 (1997).
15. J. H. J. Leclerc, Distortion-free suppression of the residual water peak in proton spectra by postprocessing, *J. Magn. Reson. B* **103**, 64–67 (1994).
16. M. Deriche and X. Hu, Elimination of water signal by postprocessing, *J. Magn. Reson.* **101**, 229–232 (1993).
17. K. Roth, B. J. Kimber, and J. Feeney, Data shift accumulation and alternate delay accumulation techniques for overcoming the dynamic range problem, *J. Magn. Reson.* **41**, 302–309 (1980).
18. P. Christiansen, O. Henriksen, M. Stubgaard, P. Gideon, and H. B. Larsson, In vivo quantification of brain metabolites by ^1H -MRS using water as an internal standard, *Magn. Reson. Imaging* **11**(1), 107–118 (1993).
19. J-P. Antoine, A. Coron, and J-M. Dereppe, Water peak suppression: Time-frequency vs timescale approach, *J. Magn. Reson.* **144**, 189–194 (2000).
20. H. Serrai, L. Senhadji, D. B. Clayton, and J. D. de Certaines, Evaluation of the continuous wavelet transform as a potential method for postacquisition water suppression in biomedical proton magnetic resonance spectroscopy, *Spec. Lett.* **33**(1), 47–67 (2000).
21. H. Serrai, L. Senhadji, J. D. de Certaines, and J. L. Coatrieux, Time-domain quantification of amplitude, chemical shift, apparent relaxation time T_2^* , and phase by wavelet-transform analysis: Application to biomedical magnetic resonance spectroscopy, *J. Magn. Reson.* **124**, 20–34 (1997).
22. A. Grossmann and J. Morlet, Decomposition of Hardy functions into square integrable wavelets of constant shape, *SIAM J. Math. Anal.* **15**, 723–736 (1984).
23. A. Grossmann, R. Kronland-Martinet, and J. Morlet, in “Wavelets” (J. M. Combes, A. Grossmann, and Ph. Tchamitchian, Eds.), p. 1, Springer-Verlag, Marseille, 1989.
24. Ph. Guillemain Ph., R. Kronland-Martinet, and B. Martens, in “Wavelets and Applications” (Y. Meyer, Ed.), p. 39, Masson, Paris, 1989.
25. H. Serrai, L. Nadal, M. Le Floch, G. Leray, L. Senhadji, N. Le Tallec, and J. D. de Certaines, Wavelet transform in magnetic resonance data processing: Application to subtraction of broad resonances, resolution of overlapping peaks and quantification. *J. Magn. Reson. Anal.* **3**, 79–86 (1997).
26. H. Serrai, A. Borthakur, L. Senhadji, R. Reddy, and N. Bansal, Time-domain quantification of multiple-quantum-filtered ^{23}Na signal using continuous wavelet transform analysis, *J. Magn. Reson.* **142**, 341–347 (2000).
27. H. Serrai, L. Nadal, H. Poptani, J. D. Glickson, and L. Senhadji, Lactate editing and lipid suppression by continuous wavelet transform analysis: Application to simulated and ^1H MRS brain tumor time-domain data, *Magn. Reson. Med.* **43**, 649–656 (2000).
28. H. Serrai, D. B. Clayton, L. Senhadji, Z. Chun, and R. E. Lenkinski, Localized proton spectroscopy without water suppression: An analytical solution for the removal of gradient induced frequency modulations, Submitted.
29. V. Govindaraju, K. Young, and A. A. Maudsley, Proton NMR chemical shifts and coupling constants for brain metabolites, *NMR Biomed.* **13**, 129–153 (2000).
30. H. Serrai, L. Nadal, G. Leray, B. Leroy, B. Delplanque, and J. D. de Certaines, Quantification of plasma lipoprotein fractions by wavelet transform time-domain data processing of proton nuclear magnetic resonance methylene spectral region, *NMR Biomed.* **11**, 273–280 (1998).